

Research Article

Experiments with a LoRaWAN-Based Remote ID System for Locating Unmanned Aerial Vehicles (UAVs)

Ali Ghubaish , Tara Salman, and Raj Jain

Computer Science & Engineering, Washington University in St. Louis, St. Louis 63130, USA

Correspondence should be addressed to Ali Ghubaish; aghubaish@wustl.edu

Received 24 May 2019; Revised 19 September 2019; Accepted 26 September 2019; Published 20 October 2019

Guest Editor: Zeeshan Kaleem

Copyright © 2019 Ali Ghubaish et al. This is an open access article distributed under the Creative Commons Attribution License, which permits unrestricted use, distribution, and reproduction in any medium, provided the original work is properly cited.

Federal Aviation Administration (FAA) of the United States is considering Remote ID systems for unmanned aerial vehicles (UAVs). These systems act as license plates used on automobiles, but they transmit information using radio waves. To be useful, the transmissions in such systems need to reach long distances to minimize the number of ground stations to capture these transmissions. LoRaWAN is designed as a cheap long-range technology to be used for long-range communication for the Internet of Things. Several manufacturers make LoRaWAN modules, which are readily available on the market and are, therefore, ideal for the UAVs Remote IDs at a low cost. In this paper, we present our experiences in using LoRaWAN technology as a communication technology. Our experiments to identify and locate the UAV systems uncovered several issues of using LoRaWAN in such systems that are documented in this paper. Using several ground stations, we can determine the location of a UAV equipped with a LoRaWAN module that transmits the UAV Remote ID. Hence, it can help identify UAVs that unintentionally, or intentionally, fly into restricted zones.

1. Introduction

According to the Federal Aviation Administration (FAA), around seven million unmanned aerial vehicles (UAVs) will be sold in the United States by 2020 [1]. UAVs have great potential in many civilian and military applications. Nevertheless, they can hinder public safety and privacy when flying in unauthorized areas. Governments may restrict or forbid UAVs flying in certain areas without prior permission. Such areas include airports, borders, and many others. In 2016 alone, around 1,800 violations were reported, including UAVs approaching airplanes and disturbing their safety [2–4]. This number has increased by more than one-third compared to 2015. Although no catastrophic accident has happened, it is essential to find a solution to reduce these violations.

Many solutions have been proposed for UAV surveillance such as the mandatory registrations in the FAA registry, geolocation systems, drone guns, signal jammers, sound recognition systems, and visual perception systems. The FAA started a UAV registry in 2015 to locate the owners

of UAVs violating any rules [5, 6]. UAV manufacturers use the global positioning system (GPS), which is a satellite-based navigation system owned by the United States, to detect the UAV's location and prevent it from flying in restricted areas [7, 8]. Two drone guns, “Dronegun” and “DroneDefender,” have been offered by two different companies to bring down UAVs causing problems [9, 10]. These guns are used to override the signal between the UAV and its remote control, and the UAV is then controlled by the gun controller. However, drone guns require the UAV to be in the line of sight (LoS) of a human with the gun to find the same frequency used by the UAV's remote control to control it. Signal jammers have been used to prevent UAVs from being controlled by their owners when the UAVs enter restricted areas. This forces the UAVs to go back to their configured home point if they lose their control signal. However, jamming affects other wireless devices that use the same frequency band that the UAVs use. This includes 2.4 GHz used by Wi-Fi, which makes this approach inconvenient in most places. UAVs can also be detected by their propeller sound; hence, two different UAV sound

recognition systems were purposed by Shi et al. and Anwar et al. [11, 12]. The issue with these systems is that it may not efficiently work if an audio jammer device is attached to the UAV. Visual perception systems like humans' vision, cameras, and proper monitoring may be easier to enforce security in the restricted areas, but these come with cost and maintenance difficulties.

One of the solutions that are being considered by the FAA is to require all the UAVs to have a Remote ID [13, 14]. These IDs will serve as license plates that transmit information to allow authorities to determine the owners of the UAVs and may detect their locations. Remote ID transmission needs a long-haul wireless technology that is cheap enough for low-cost UAVs but still reaches several miles. We believe LoRaWAN is one such technology that can reach from 9 to 18 miles (15 to 30 kilometers) in optimal cases [15, 16]. Hence, deploying a system that uses LoRaWAN protocol can help track the UAVs.

We have developed a prototype and have experimented with LoRaWAN protocol on UAVs. Our goal was to find the feasibility of using this protocol to locate and identify the UAVs. Finding the location of any UAV required us to determine the 3-dimensional (3-D) location of the UAV using several ground stations (GSs) listening to the ID broadcasts from the UAV. Upon reception, each GS estimates the distance between itself and the UAV. A minimum of four GSs are required to estimate the location of the UAV in 3-D. A system like this can help law enforcement to be alerted when any UAV flies in a restricted area. We found several issues with using the LoRaWAN protocol in such systems. These issues include the variability of using different LoRaWAN modules, the module's antenna direction, and the battery capacity to run these modules.

The rest of the paper is organized as follows: Section 2 provides background and related work; Section 3 discusses system architecture; and Section 4 shows the experimental implementation and results in detail. The critical issues discovered by our experiments are discussed in Section 5. Finally, conclusions and future work are presented in Section 6.

2. Background and Related Work

This section gives a brief background on the technologies used in the paper. Besides, we discuss some of the earlier related works.

2.1. LoRaWAN. A UAV is controlled by a ground-based remote controller via a radio frequency (RF) communication protocol [17]. RF technologies such as LoRaWAN, Zigbee, and 6LoWPAN can be used for communications [18–21]. LoRaWAN is a relatively new technology that is suitable for UAV communications due to its low power, low cost, and long-range reachability. The medium access control (MAC) protocol for LoRaWAN has been standardized by the LoRa Alliance. It uses the LoRa physical layer that enables it to reach long ranges with low-power consumption using the chirp spread spectrum modulation [18, 22]. We selected

LoRaWAN for location estimation due to its low cost and long-range reachability. Further description of LoRaWAN can be found in [15].

2.2. Distance and Location Estimation. Different methods have been explored in the literature for distance estimation. These methods include the time of arrival (ToA), time of flight (ToF), and received signal strength indication (RSSI) [23–26]. ToA method uses elapsed time between sending and receiving a signal between two nodes to measure the distance between them. For instance, GPS uses the ToA between a client node and a satellite to measure the distance between them [8]. The ToF method measures the time for radio signals to bounce back to the GS after being sent to the UAV. This method has been used in aircraft since 1950 [27].

RSSI is a measure of the quality of the signal and can be used for distance estimation. It measures the power level of the received signal [28]. Its value is measured in decibel (dB) and has multiple applications in wireless communication. One of these applications is distance estimation between two nodes, such as the UAV and the GS [29].

Location estimation of any UAV requires knowing its distance from several GSs with known coordinates. For locating the UAV in 2-dimension (2-D), distances from at least 3 GSs are required. For location estimation in 3-D, distances from four GSs are required. Given the coordinates of the required number of GSs and by estimating the distance using one of the previously stated methods, the location of the UAV can be estimated. For example, the ToA method is being used in GPS, which consists of around 31 satellites [8]. Each satellite broadcasts its location and time. By knowing how far the UAV is from one satellite, the UAV knows its distance from that satellite and knows that it is located on a sphere with the estimated distance as a radius. Adding at least two more satellites' information can help the UAV estimate its location in 2-D by finding the points where the three satellites' spheres intersect. Further, adding more satellites' information to the equation can pinpoint the UAV's location and reduce the uncertainty (error) to a few meters.

2.3. Related Work. Most prior works in UAV location estimation use GPS. UAVs can be used for many applications such as delivering products and acting as a flying ad-hoc network for broadband wireless access during emergencies [30–32]. Most of these applications need to know the location of the UAV, and they use GPS coordination for that. However, GPS is not always available and not usable for identification. Thus, investigating other alternative localization solutions with an identification feature is desirable for UAV localization in all applications.

Wang et al. investigate a UAV rescue system, named GuideLoc, that helps to rescue people during a natural disaster using UAVs [33]. GuideLoc captures the average RSSI value of a wireless device signal such as a mobile phone carried by a trapped person. The system uses the antennas attached to the UAV to capture the average RSSI value. If the average RSSI value is less than a threshold, the angle of

arrival of the signal gets updated to find the location of that person and to record the GPS coordinates of the trapped person. The angle of arrival is determined by the strength of the average RSSI value. Lee et al. utilize the same technique to localize the sensor nodes in the wireless sensor networks [34]. Our system differs from GuideLoc by relying only on the RSSI values to estimate the UAV location and not the GPS.

Raimundo et al. examine the possibility of using the LoRaWAN communication protocol for a UAV location system [35]. The system consists of a UAV that uses a global navigation satellite system (GNSS) receiver to gather the GNSS data and then sends them by a LoRaWAN module attached to the UAV. GNSS receivers can connect to different satellite-based systems such as GPS and other navigation systems [36]. The LoRaWAN module sends the GNSS positions to a base station on the ground. In our system, the UAV is located and identified using the RSSI values and a message that is broadcasted using the LoRaWAN technology.

UAVs have been used by Ferreira et al. to find the network distribution and coverage in remote areas or hazard locations [37]. The proposed system uses the UAV's center-modem to detect the network access points (APs) using the RSSI values broadcasted by the APs in the network. The system uses these RSSI values to estimate the AP locations based on known UAV locations in different reference points, during the UAV flying path, and the estimates distance to these APs. The free-space propagation model is utilized in the system for distance estimation, and three different location methods are tested [38]. They conclude that Bound Box method has the lowest estimation error with a low variance when increasing the number of reference points. Another system by Greco et al. is similar to that by Ferreira et al., but they rely on radio-frequency identification (RFID) tags instead of APs to be located by the UAVs [39].

One of the issues facing location-based systems is to locate objects or UAVs in indoor environments. Tian et al. introduce the HiQuadLoc system that uses Wi-Fi access points to locate a UAV in an indoor environment [40]. Twenty APs are utilized in the system in an area of 1100 m². The system uses two phases: an offline phase and an online phase. The offline phase divides the indoor area into cubes with known RSSI values to correctly help detect the UAV location in the online phase. The system achieves an average error of 1.64 m. The UAV speed is varied up to three meters per second. They conclude that the location error increases as the UAV speed increases.

Cheng et al. propose a system that can locate a nonline of sight (NLOS) UAV in an indoor environment [41]. The system uses RSSI values in the NLOS identification algorithm to identify the propagation conditions. Also, they use particle swarm optimization-based maximum joint probability algorithm to find the UAV's 2-D coordinates. The system achieves an average error of 0.85 m.

Our system also uses RSSI values for distance estimation; however, we target outdoor environments rather than indoors, and we use LoRaWAN to allow location estimation over much longer distances.

3. System Architecture

In this section, the system components, distance estimation modeling, and location estimation for the RSSI method are discussed. The discussion also includes the modeling methods used to estimate the distance from the RSSI values, along with graphs that illustrate that method.

3.1. Prototype Components. As shown in Figure 1, our prototype system consists of five main components: LoRaWAN modules, GSs, antennas, a battery, and a UAV. In the following, we briefly discuss these components:

- (i) *LoRaWAN Modules.* Two different modules are used—Moteino LoRa and Seeeduino LoRaWAN—for our prototype, as shown in Figure 1. Seeeduino module uses 433/868 MHz frequency bands while the Moteino module uses the 915 MHz band. Both modules can report the RSSI values while the Moteino module has an external antenna for longer ranges. The details of these modules can be found in [42, 43]. Alternatively, we could have used Libelium LoRaWAN module [44]. However, we have used Seeeduino and Moteino as shown in the distance estimation modeling since they meet our requirements such as reporting RSSI values where Libelium module lacks this feature.
- (ii) *GS.* For each GS, we use a regular computer connected to a LoRaWAN module. The computer is used to program the LoRaWAN module and record the data.
- (iii) *Antenna.* Moteino LoRa module requires a separate directional antenna to work, while the Seeeduino LoRaWAN module has a built-in wire antenna on the module.
- (iv) *Battery.* Any power bank is sufficient to power the LoRaWAN module connected to the UAV.
- (v) *UAVs.* We use two different UAVs for the prototype: DJI Phantom 2 and DJI Phantom 4 Pro. As discussed earlier, a LoRaWAN module and a battery have been attached to each UAV.

3.2. Modeling for Distance Estimation. Using the configuration shown in Figure 1, we estimate the distance between one of the GSs and the UAV using the RSSI values, and the log-distance path loss model as will be discussed. For each LoRaWAN module, two modules are used: one is attached to the UAV and powered by a battery and the other is connected to a computer to control and record the data and serves as the GS.

For distance estimation, the UAV continuously broadcasts a message that has its ID. The interval time of successive messages is two seconds, which is the minimum interval time for the LoRaWAN modules to avoid losing messages [45]. The message length and its effect are explained later in Section 4.

The log-distance path loss model states that [46]

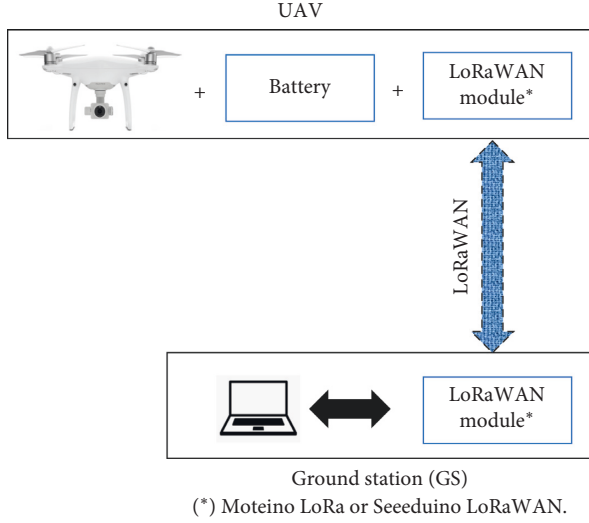


FIGURE 1: System architecture for distance estimation. Two LoRaWAN modules, Moteino and Seeeduino LoRaWAN, are used for distance estimation.

$$\text{RSSI} = -10 * L * \log_{10}(d) - C, \quad (1)$$

where RSSI is the RSSI value measured at the destination, d is the distance, L is the path loss exponent, and C is a constant. Given (1), the distance between the UAV and the GS can be measured as follows:

$$d = 10^{-((\text{RSSI}-C)/10L)}. \quad (2)$$

However, the measured RSSI values can fluctuate, and thus, using one value is not sufficient to estimate the distance. Typically, multiple values need to be used. In our experiments, we used an average of five RSSI values to measure the distance. Five is chosen arbitrarily as a tradeoff between the time and the fluctuation in the RSSI values.

That is, the distance between a GS and the UAV can be estimated as follows:

$$d = 10^{-((\text{meanRSSI}-C)/10L)}. \quad (3)$$

Here, meanRSSI is the average RSSI value of five RSSI values.

Even though C and L are constants in (1), their values are initially unknown and depend on the environment, as discussed by Sherazi et al. [47]. To estimate these parameters, we need meanRSSI values and their corresponding distances for a few known positions. Therefore, a model is needed to estimate these values using (1). To do so, we fit a linear model to the meanRSSI values. In the resulting linear model, the slope is $-10 * L$ (thus, $L = -\text{slope}/10$), and it can be calculated as follows:

$$\text{slope} = \left(\frac{\sum xy - n\bar{x}\bar{y}}{\sum x^2 - n\bar{x}^2} \right), \quad (4)$$

where x is the meanRSSI value at a known position or a known distance, y is the $\log_{10}(d)$ value corresponding to the meanRSSI value, n is the number of RSSI values included in

that mean, and \bar{x} and \bar{y} are the mean over all meanRSSI values and the mean over all $\log_{10}(d)$ values, respectively.

In the resulting linear model, the intersection point is $-C$ (thus, $C = -\text{intersection}$) which can be calculated from the linear model as follows:

$$\text{intersection} = \bar{y} - \text{slope} \times \bar{x}. \quad (5)$$

To get the distances between the UAV and the GS, we tried to use a laser meter to measure the distance between the two ends. However, it becomes difficult to do such measurements when the actual distance gets above 200 m. In such a case, the UAV gets smaller and harder to detect by the laser meter. Hence, as shown in Figure 2, we measure the ground distance (GD) between a ground point (GP) and the GS to compute the slant distance (SD) between the GS and the UAV, which equals d in (3). The measurement is relatively accurate, as will be shown in Section 4. The slant distance can be estimated as follows [48]:

$$\text{SD} = \sqrt{\text{GD}^2 + H^2 - (2 * \text{GD} * H * \cos(\beta))}, \quad (6)$$

where H is the height of the UAV, which is set to 50 m, GD is the ground distance between the GP under the UAV and the GS, and β is the angle between the GS and the UAV. The height is fixed to take the distance as the only variable parameter to simplify the measurements. The GD and its corresponding angle are measured using the laser meter. The GP is selected to be directly below the UAV. Thus, the angle between the UAV and the GP is 90 degrees, and it is measured using the laser meter, which is attached to a tripod. The angle α between the GP and the GS is measured with the laser meter. Note that, β can be calculated by subtracting α from 90 degrees:

$$\beta = (90 - \alpha). \quad (7)$$

Using the above technique, one can estimate the values for the parameters C and L . These parameters can then be used with the measured meanRSSI value to estimate distances at other UAV positions.

3.3. Location Estimation. In the first stage of our experiments, the Seeeduino LoRaWAN module is used to estimate the location of the UAV using the RSSI method. The location system consists of four GSs and one UAV, as illustrated in Figure 3.

Seeeduino LoRaWAN module is attached to each of the GSs and the UAV. In addition, a battery to power the LoRaWAN module is also attached to the UAV. In each GS, there is a computer that records the meanRSSI values received from the module connected to it. In this stage, the data are manually collected from all the four GS computers and transferred to a fifth computer called the central computer, which is not shown in Figure 3. The transferred data are processed based on three elements: the GSs' 3-D locations, the distances between each of the four GSs, which is 200 m, and the meanRSSI values received from the four GSs.

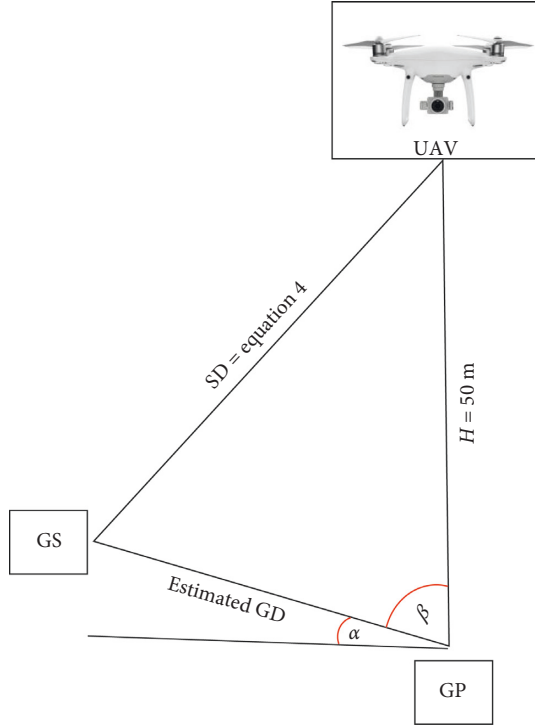


FIGURE 2: Slant-distance estimation technique. This technique is used if the distance between the two nodes is larger than 200 m.

The location estimation uses the SD between the UAV and four GSs. As explained earlier, the Seeeduino module requires an interval time of two seconds between successive messages. To satisfy this requirement and that we need to use the mean of 5 RSSI values, the UAV must stay in one spot for at least 10 seconds. Trilateration technique is used to determine the location of the UAV [49, 50]. This technique has been used to estimate the location in [51–53]. It allows us to determine the exact 3-D location of any object using its distance from at least four points with their known 3-D locations. In our case, the UAV is the object whose location and height need to be determined, while the four GSs are the points with known locations, as shown in Figure 4.

The UAV is on the surface of a sphere with radius (r_i) centered at GS_i . The r_i is equal to SD_i for each GS. The location of the UAV is a 3-element vector $\mathbf{w} = \{x, y, z\}$. It can be computed as the intersection of the four spheres. Each sphere consists of the 3-D location of each GS and the radius value between itself and the UAV. The radius value represents the estimated distance, SD, from the previous subsection. Therefore,

$$\begin{aligned} r_1^2 &= (x - x_1)^2 + (y - y_1)^2 + (z - z_1)^2, \\ r_2^2 &= (x - x_2)^2 + (y - y_2)^2 + (z - z_2)^2, \\ r_3^2 &= (x - x_3)^2 + (y - y_3)^2 + (z - z_3)^2, \\ r_4^2 &= (x - x_4)^2 + (y - y_4)^2 + (z - z_4)^2. \end{aligned} \quad (8)$$

We can expand out the squares in each one, as shown in the following equation:

$$\begin{aligned} r_1^2 &= x^2 - 2x_1x + x_1^2 + y^2 - 2y_1y + y_1^2 + z^2 - 2z_1z + z_1^2, \\ r_2^2 &= x^2 - 2x_2x + x_2^2 + y^2 - 2y_2y + y_2^2 + z^2 - 2z_2z + z_2^2, \\ r_3^2 &= x^2 - 2x_3x + x_3^2 + y^2 - 2y_3y + y_3^2 + z^2 - 2z_3z + z_3^2, \\ r_4^2 &= x^2 - 2x_4x + x_4^2 + y^2 - 2y_4y + y_4^2 + z^2 - 2z_4z + z_4^2. \end{aligned} \quad (9)$$

By subtracting the 4th equation (r_4) from the first three equations in (9), we get the following:

$$\begin{aligned} 2(x_4 - x_1)x + 2(y_4 - y_1)y + 2(z_4 - z_1)z \\ &= r_1^2 - r_4^2 - x_1^2 - y_1^2 - z_1^2 + x_4^2 + y_4^2 + z_4^2, \\ 2(x_4 - x_2)x + 2(y_4 - y_2)y + 2(z_4 - z_2)z \\ &= r_2^2 - r_4^2 - x_2^2 - y_2^2 - z_2^2 + x_4^2 + y_4^2 + z_4^2, \\ 2(x_4 - x_3)x + 2(y_4 - y_3)y + 2(z_4 - z_3)z \\ &= r_3^2 - r_4^2 - x_3^2 - y_3^2 - z_3^2 + x_4^2 + y_4^2 + z_4^2. \end{aligned} \quad (10)$$

Putting (10) in a matrix form, we get (11) where \mathbf{A} is the coefficient matrix, \mathbf{w} is a vector of variables to be estimated, i.e., (x, y, z) in (10), and \mathbf{b} is the right-side vector.

$$\begin{bmatrix} 2(x_4 - x_1) & 2(y_4 - y_1) & 2(z_4 - z_1) \\ 2(x_4 - x_2) & 2(y_4 - y_2) & 2(z_4 - z_2) \\ 2(x_4 - x_3) & 2(y_4 - y_3) & 2(z_4 - z_3) \end{bmatrix} \begin{bmatrix} x \\ y \\ z \end{bmatrix} = \begin{bmatrix} r_1^2 - r_4^2 - x_1^2 - y_1^2 - z_1^2 + x_4^2 + y_4^2 + z_4^2 \\ r_2^2 - r_4^2 - x_2^2 - y_2^2 - z_2^2 + x_4^2 + y_4^2 + z_4^2 \\ r_3^2 - r_4^2 - x_3^2 - y_3^2 - z_3^2 + x_4^2 + y_4^2 + z_4^2 \end{bmatrix} \quad (11)$$

$\mathbf{A} \quad \mathbf{w} = \quad \mathbf{b}$

Note that \mathbf{w} is the UAV 3-D location that we need to determine given other values in (11). To find \mathbf{w} , the closed-form of the least squares method can be used to solve the equation in one step, as shown in the following equation:

$$\mathbf{w} = (\mathbf{A}^T \mathbf{A})^{-1} \mathbf{A}^T \mathbf{b}. \quad (12)$$

If the height for all the GSs is the same, the last column of matrix \mathbf{A} will be all zeros, and the matrix becomes non-invertible. This step can be taken care of by removing the last column of matrix \mathbf{A} , computing only x and y values from the above equations, and separately determining z as in (13) by substituting z_4 value in (8) with zero and solving for z . Here, z represents the height of the UAV, while x and y represent the 2-D location of the UAV.

$$z = \sqrt{r_4^2 - (x - x_4)^2 - (y - y_4)^2}. \quad (13)$$

4. Experimental Implementation and Results

In this section, the experimental implementation and results are discussed. We present the steps to prepare the software and hardware for the experiments. Also, we show some statistical results for the location estimation method.

4.1. Distance Estimation Using RSSI Method. Two different outdoor environments were used to model and validate our experiments. All the nodes in the experiment used the Seeeduino LoRaWAN module, which is based on Arduino Zero bootloader with LoRaWAN protocol embedded in it;

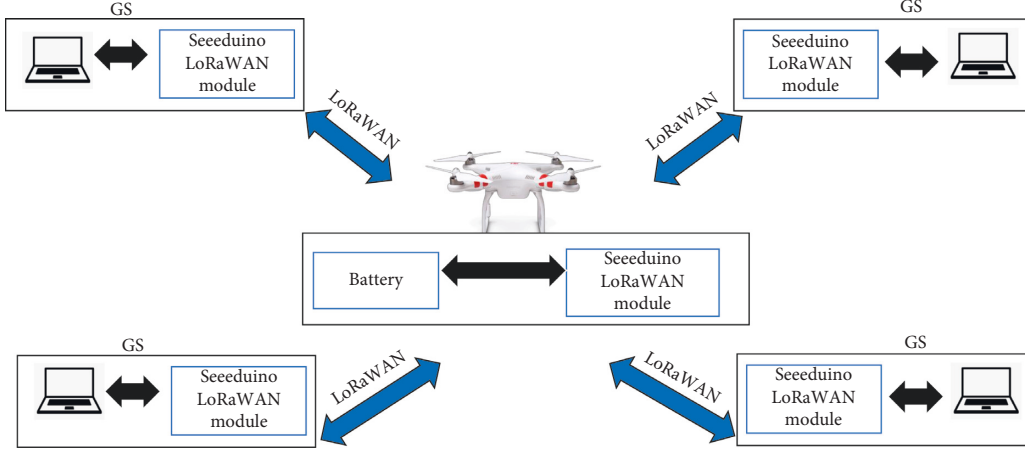


FIGURE 3: System architecture for the location estimation.

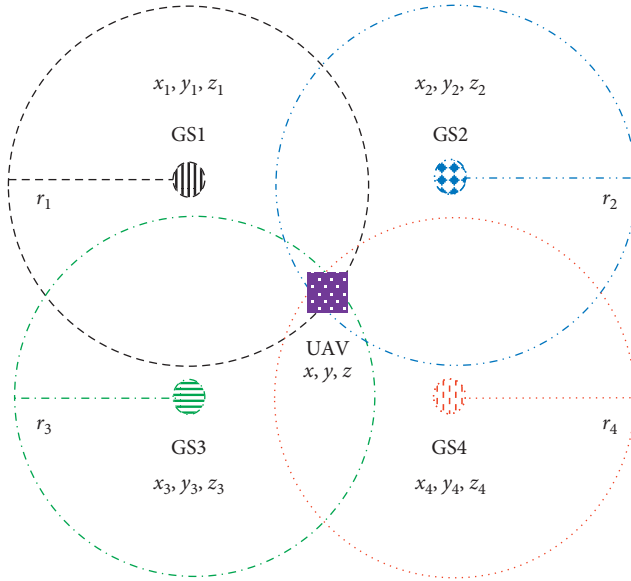


FIGURE 4: Trilateration system architecture. A minimum of four GSs 3-D locations are required to find the UAV 3-D location.

thus, no additional module was needed [43]. Seeeduino provides a library and examples to use their module. Using these examples, we found that it is possible to vary the contents and formats of the transmitted messages. Hence, three messages with different lengths and formats were tested, as shown in Table 1.

Initially, our test was based on using two nodes mounted on two tripods and not attached to the UAV with distances ranging from 100 to 500 m. As shown in Figure 5, we fitted a linear model to show the relationship between a set of meanRSSI values and their corresponding distances using different message lengths. Also, we calculated the confidence interval for each distance and message length to see if different meanRSSI values for different distances use one message overlap or not. From Figure 5, we can see that as the message length gets larger, the meanRSSI value increases. This finding is essential since with lower meanRSSI values, different distances

using different meanRSSI values overlap, causing a significant error in distance estimation. For example, by using message 2 (M2), we may get a meanRSSI value that could be 100 to 300 m away, resulting in an error of 200 m. Based on this realization, the most extended message among the three messages, M3, was used with the Seeeduino LoRaWAN module to complete the rest of this experiment.

For the second stage, we calculated the SDs for six different positions with nominal distance ranging from 100 to 600 m, as shown in Table 2. The SD values were those computed using (6). Notice that the calculated SDs were close to the nominal distances.

After getting the SDs, we performed a statistical analysis on the collected data, as shown in Table 3 using the methods described in [54]. The measurements consist of six meanRSSI values, each of which consists of 125 samples in each of the six distance ranges. Initially, the height for the UAV was fixed to 50 m to keep the analysis simple. Then, we conducted another experiment to check if the meanRSSI values were the same for different heights up to 100 m. Then, we decreased the GD and correspondingly we increased the UAV height to keep the same SD. Results showed that the meanRSSI values were the same as long the SDs were the same; that is, the meanRSSI values were not affected by the height.

As shown in Table 3, the sample variance decreased as the distance increased. To find the two unknown parameters, L and C , we used the linear regression model discussed earlier in Section 3.2. The results are shown in Figure 6. Note the decreasing variance (and hence narrower confidence interval) as the distance between the UAV and the GS increases. Overall, the model resulted in an R^2 value of 97%, which showed that the linear regression model was a good fit.

The confidence interval is essential to see if any meanRSSI value for any distance was overlapping with another meanRSSI value. After calculating these confidence intervals, we found that their values for 300/400 m values overlap. This overlap showed that the meanRSSI values for these two distances were not statistically different. In other words, given a meanRSSI value and the calculated L and C , we may estimate the distance with an error of 100 m, which

TABLE 1: Different message lengths and formats list.

#	Message	No. of bytes	Format
M1	FF 31	2	Hexadecimal
M2	FF1	3	String
M3	FF1 is the UAV ID number that is being used to identify this UAV	66	String

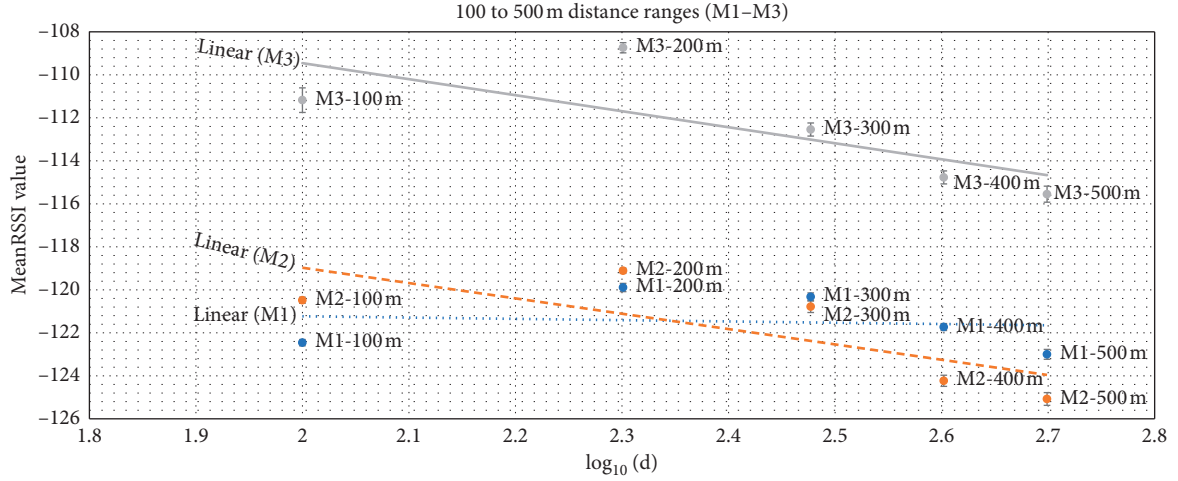


FIGURE 5: MeanRSSI values for different message lengths at different distances.

TABLE 2: Calculated SDs.

Nominal distance	Ground distance (GD)	Height (H)	UAV-GS angle (β)	GP-GS angle (α)	Slant distance (SD)
100 m	100.0 m	50 m	79.1°	10.9°	102.97 m
200 m	200.2 m	50 m	81.7°	8.3°	199.19 m
300 m	299.8 m	50 m	83.3°	6.7°	298.19 m
400 m	400.3 m	50 m	84.0°	6.0°	398.15 m
500 m	500.5 m	50 m	84.7°	5.3°	498.34 m
600 m	600.7 m	50 m	84.9°	5.1°	598.29 m

TABLE 3: Statistical characteristics of meanRSSI values using the Seeeduino LoRaWAN module.

Nominal distance	100 m	200 m	300 m	400 m	500 m	600 m
Sample variance	4.78	2.34	2.62	1.46	1.30	1.22
Sample standard deviation	2.19	1.53	1.62	1.21	1.14	1.10
Sample standard error	0.20	0.14	0.14	0.11	0.10	0.10
Sample mean (\bar{x})	-79.41	-82.94	-85.81	-85.58	-87.93	-88.32
95% confidence interval	(-79.79, -79.03)	(-83.21, -82.68)	(-86.09, -85.52)	(-85.79, -85.37)	(-88.13, -87.73)	(-88.52, -88.13)
L				1.165		
C				-56.134		
R ²				0.97		

is a drawback. At this point, we decided to check the meanRSSI value with the other LoRaWAN modules (i.e., Moteino LoRaWAN).

As shown in Table 4, the Moteino module produced meanRSSI values for different distances that overlap with other distance ranges from 100 to 800 m; hence, it is not a perfect candidate for the linear regression model to find L and C parameters. We found that the perfect length of the message for the Moteino module was M2 (shown earlier in Table 1).

Longer messages, e.g., M3, were transmitted in several fragments. Hence, we ended up using M2 instead of M3.

4.2. Location Estimation Using RSSI Method. Location estimation stage consisted of four GSs and one UAV. The UAV used in this stage was DJI Phantom 4. The GSs were 200 m away from each other where all antennas' directions were pointing up since that impacts the meanRSSI values,

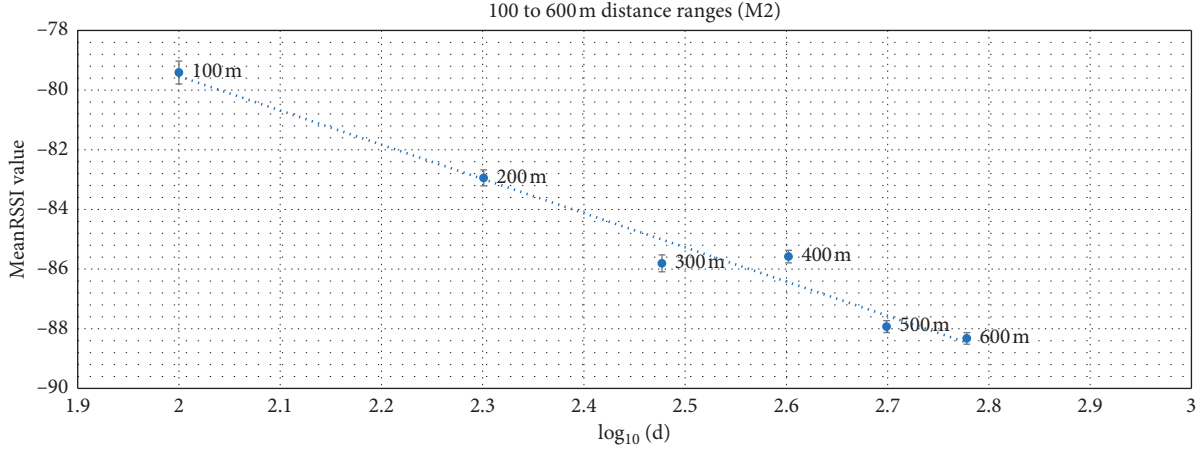


FIGURE 6: Linear regression model. These measurements are based on the use of the Seeeduno LoRaWAN module.

TABLE 4: Statistical characteristics of meanRSSI values using the Moteino LoRaWAN module.

Distance	100 m	200 m	300 m	400 m	500 m	600 m	700 m	800 m
Sample mean	-104.48	-103.68	-103.51	-104.97	-105.06	-104.86	-104.62	-104.65
Confidence interval	(-104.61, -104.36)	(-103.81, -103.55)	(-103.61, -103.40)	(-105.03, -104.90)	(-105.11, -105.00)	(-104.93, -104.80)	(-104.72, -104.52)	(-104.75, -104.56)

according to Wadhwa et al. [55]. The UAV antenna had a spring shape facing down, as shown in Figure 7. The battery that was used to power-up the LoRaWAN module attached on the UAV was under the module itself as shown in the figure.

The measured and estimated SD with UAV at the height of 50 m are shown in Table 5. The real SDs were measured using the GPS, while the estimated SDs were based on the meanRSSI values.

After we calculated the distance error based on the difference between the estimated SDs and real SDs, we found that GS2 showed a distance error of 127%. This error is discussed further in the next section.

5. Issues and Challenges

Although LoRaWAN can be used for distance estimation using RSSI method, we run into several issues that are important and are the main results of this paper. These are

- (1) *LoRaWAN Module*. LoRaWAN is designed for low cost and; therefore, there is significant variability in the results using different modules. Each module has its peculiarities. Further work is required to make either a standard module for consistent results or a standard that when implemented by different manufactures results in similar results.
- (2) *RSSI Model Accuracy*. MeanRSSI values fluctuate and depend upon the LoRaWAN module. As shown in Figure 6, our distance estimation model could be considered accurate except at distances between 300 and 400 m. Designing a better method or using a better module can resolve this problem.

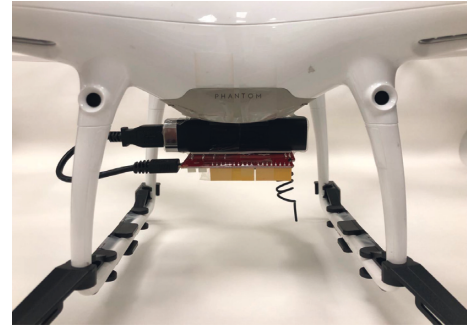


FIGURE 7: Seeeduno LoRaWAN module with the battery attached to the UAV. The shape of the antenna and the battery location is essential since the meanRSSI values are affected by them.

TABLE 5: Statistical characteristics of location determination using the Seeeduno LoRaWAN module.

	GS1	GS2	GS3	GS4
MeanRSSI (dB)	-80	-86	-79	-81
Estimated SD (m)	112	366	92	136
Real SD ¹ (m)	146	161	140	155
Distance error ² (%)	23	127	34	12

¹Using Google Maps “measure distance” feature. ²The error is calculated based on the difference between the estimated SDs and real SDs.

- (3) *Battery Capacity*. Different battery capacities to run the UAV’s LoRaWAN module cause different meanRSSI values for short distances (below 300 m); hence, we recommend using the same battery capacity throughout the whole set of measurements.
- (4) *Antenna Direction*. The module antenna direction and position affect the meanRSSI values captured by

the GSs. Thus, when building the distance model, the position and direction of the antenna need to be fixed for all UAVs during the distance estimation modeling and location estimation stage. Otherwise, C and L factors will change, resulting in inaccurate estimation of the distances, and thus, wrong locations.

- (5) *Seeeduino LoRaWAN Module Power Cable*. We found that the cable used to provide the power to the module attached to the UAV should be in the opposite direction of the antenna to balance the power in all directions. This issue is due to the fact that the cable can act as a second antenna for the Seeeduino LoRaWAN module, which affects the meanRSSI values for the modules in that direction of the UAV.
- (6) *Battery Location*. The battery used with the LoRaWAN module attached to the UAV needs to be under the module; otherwise, the meanRSSI values will be higher from the battery side, resulting in inaccurate distance estimation models.
- (7) *Environments*. Different environments affect the meanRSSI values because the model is based on a specific environment. This factor also results in different L and C values and thus different distance estimation models. As a result, the values of L and C need to be calibrated to fix the difference in the meanRSSI value between the two environments.
- (8) *Modeling Range*. The meanRSSI values for shorter distances (less than 100 m) are not useable because of their high variability. If there are GSs located throughout a city, some GSs will be more than 100 m distance from a UAV; hence, it may not be a problem.
- (9) *Movement*. We had to keep the UAV stationary for at least ten seconds to get the meanRSSI value to be used for distance estimation. This factor is because our LoRaWAN module required at least two seconds interval between successive messages and we need five such messages to compute the meanRSSI value. A better module design may allow to overcome this and continuously measure the location.
- (10) *Underestimation*. In our experiments, we had the minimum number of GSs required for the 3-D location. In such cases, it is possible that the estimated distances are lower than actual, and the four spheres do not intersect. Mathematically, this shows up as a negative value under the square root resulting in “imaginary” height for the UAV.

6. Conclusions and Future Work

Remote IDs on UAVs will allow law-enforcement authorities to determine the ownership of the UAVs. Making the UAVs simply broadcasting their GPS-determined location may not be sufficient in all environments. In some situations, determining the location using the reception on ground

stations is appropriate. In this paper, we proposed LoRaWAN as one possible wireless technology to use for Remote ID transmission and showed how ground stations could use meanRSSI values to determine the 3-D location of UAVs. We developed a prototype using commercially available low-cost LoRaWAN modules to identify and locate the UAVs, and we uncovered several issues that were documented in Section 5. These are the main contributions of this paper. We plan to do further work to address these issues in the near future.

Data Availability

The LoRaWAN module configurations, Arduino IDE setups, and codes used to support the findings of this study are documented in [56].

Conflicts of Interest

The authors declare that there are no conflicts of interest regarding the publication of this paper.

Acknowledgments

I would like to thank my master thesis committee, Professor Roger Chamberlain and Ben Moseley, for their excellent comments and help to improve the overall write-up. In addition, I would like to thank my colleagues Guillaume Valentis, Xipeng Wang, Arghya Datta, Marcio Teixeira, Maede Zolanvari, Ria Das, and Yousef AlShehri for their help in this paper. Ali Ghubaish was financially supported by Prince Sattam bin Abdulaziz University, AlKharj 11942, Saudi Arabia.

References

- [1] Federal Aviation Administration, *FAA Releases 2016 to 2036 Aerospace Forecast*, 2016, <https://www.faa.gov/news/updates/?newsId=85227>.
- [2] W. Bellamy III, *Drones Came Too Close to Airplanes 1,800 Times in 2016*, 2017, <http://www.aviationtoday.com/2017/03/17/drones-came-close-airplanes-1800-times-2016/>.
- [3] M. Zanova, “Drone sightings near airplanes on the rise,” 2017, <http://thehill.com/policy/transportation/362556-drone-sightings-near-airplanes-on-the-rise>.
- [4] C. Shine, “FAA playing high-tech hide and seek at DFW to stop drones from colliding with flights,” 2017, <https://www.dallasnews.com/business/dfw-airport/2017/04/28/1800-drone-sightings-last-year-faa-testing-systems-prevent-airport-collisions>.
- [5] Federal Aviation Administration, “Drone registration,” 2019, http://federaldroneregistration.com/?gclid=CjwKCAiAxarQBRAmEiwA6YcGKHV8CMGVSGIsDn0cSsvl4lX-n7Z4lMB3aFl9iIXuRf8Bx2p6Co7QyRoCYBcQAvD_BwE.
- [6] Wikipedia, “Regulation of UAVs in the United States,” 2019, https://en.wikipedia.org/wiki/Regulation_of_UAVs_in_the_United_States.
- [7] DJI, “DJI introduces new geofencing system for its drones,” 2015, <https://www.dji.com/newsroom/news/dji-fly-safe-system>.
- [8] Wikipedia, *Global Positioning System*, 2019, https://en.wikipedia.org/wiki/Global_Positioning_System.

- [9] K. D. Atherton, "This device turns any gun into an anti-drone ray," 2015, <https://www.popsci.com/dronedefender-is-an-anti-drone-rifle-attachment>.
- [10] K. D. Atherton, "This drone gun knocks drones out of the sky gently, with radio waves," 2016, <https://www.popsci.com/drone-gun-downs-drones-with-radio-waves>.
- [11] L. Shi, I. Ahmad, Y. He, and K. Chang, "Hidden Markov model based drone sound recognition using MFCC technique in practical noisy environments," *Journal of Communications and Networks*, vol. 20, no. 5, pp. 509–518, 2018.
- [12] M. Z. Anwar, Z. Kaleem, and A. Jamalipour, "Machine learning inspired sound-based amateur drone detection for public safety applications," *IEEE Transactions on Vehicular Technology*, vol. 68, no. 3, pp. 2526–2534, 2019.
- [13] Federal Aviation Administration, "UAS remote identification," 2019, https://www.faa.gov/uas/research_development/remote_id/.
- [14] J. Plaza, "FAA issues an RFI for a remote ID system for drones," 2019, <https://www.expouav.com/news/latest/faa-rfi-remote-id-drones/>.
- [15] L. Alliance, "A technical overview of LoRa® and LoRaWAN™," p. 20, 2015, https://docs.wixstatic.com/ugd/eccc1a_ed71ea1cd969417493c74e4a13c55685.pdf.
- [16] J. Rafferty, J. Synnott, A. Ennis, I. Cleland, C. Nugent, and M. Little, "A secure, out of band, mechanism to manage IoT devices," in *Proceedings of the 11th International Conference on Ubiquitous Computing and Ambient Intelligence*, vol. 10586, pp. 77–90, Philadelphia, PA, USA, November 2017.
- [17] Wikipedia, "Unmanned aerial vehicle," 2019, https://en.wikipedia.org/wiki/Unmanned_aerial_vehicle#Flight_controls.
- [18] M. Saari, A. M. b. Baharudin, P. Sillberg, S. Hyrynsalmi, and W. Yan, "LoRa—a survey of recent research trends," in *Proceedings of the 2018 41st International Convention on Information and Communication Technology, Electronics and Microelectronics (MIPRO)*, pp. 872–877, Opatija, Croatia, May 2018.
- [19] P. Kinney, "Zigbee technology: wireless control that simply works," in *Proceedings of the Communications Design Conference*, pp. 1–7, San Jose, CA, USA, September–October 2003.
- [20] W. Wang, G. He, and J. Wan, "Research on Zigbee wireless communication technology," in *Proceedings of the 2011 International Conference on Electrical and Control Engineering*, pp. 1245–1249, Yichang, China, September 2011.
- [21] Z. Yang and C. H. Chang, "6LoWPAN overview and implementations," in *Proceedings of the 2019 International Conference on Embedded Wireless Systems and Networks*, pp. 357–361, Beijing, China, February 2019.
- [22] A. Lavric and A. I. Petrariu, "LoRaWAN communication protocol: the new era of IoT," in *Proceedings of the 2018 International Conference on Development and Application Systems (DAS)*, pp. 74–77, Suceava, Romania, May 2018.
- [23] S. Schwarzer, M. Vossiek, M. Pichler, and A. Stelzer, "Precise distance measurement with IEEE 802.15.4 (Zigbee) devices," in *Proceedings of the 2008 IEEE Radio and Wireless Symposium*, pp. 779–782, Orlando, FL, USA, January 2008.
- [24] A. Savvides, C.-C. Han, and M. B. Strivastava, "Dynamic fine-grained localization in Ad-Hoc networks of sensors," in *Proceedings of the 7th Annual International Conference on Mobile Computing and Networking*, pp. 166–179, Rome, Italy, 2001.
- [25] S. Lanzisera, D. Zats, and K. S. J. Pister, "Radio frequency time-of-flight distance measurement for low-cost wireless sensor localization," *IEEE Sensors Journal*, vol. 11, no. 3, pp. 837–845, 2011.
- [26] Y. Miao, H. Wu, and L. Zhang, "The accurate location estimation of sensor node using received signal strength measurements in large-scale farmland," *Journal of Sensors*, vol. 2018, Article ID 2325863, 10 pages, 2018.
- [27] Wikipedia, "Distance measuring equipment," 2019, https://en.wikipedia.org/wiki/Distance_measuring_equipment.
- [28] Wikipedia, "Received signal strength indication," 2019, https://en.wikipedia.org/wiki/Received_signal_strength_indication.
- [29] Wikipedia, "Indoor positioning system," 2019, https://en.wikipedia.org/wiki/Indoor_positioning_system.
- [30] Amazon, "Amazon Prime Air," 2017, <https://www.amazon.com/Amazon-Prime-Air/b?node=8037720011>.
- [31] A. Jamalipour, Z. Kaleem, P. Lorenz, and W. Choi, "Special issue on amateur drone and UAV communications and networks," *Journal of Communications and Networks*, vol. 20, no. 5, pp. 429–433, 2018.
- [32] Z. Kaleem, M. Yousaf, A. Qamar et al., "UAV-empowered disaster-resilient edge architecture for delay-sensitive communication," *IEEE Network*, pp. 1–9, 2019.
- [33] A. Wang, X. Ji, D. Wu et al., "GuideLoc: UAV-assisted multitarget localization system for disaster rescue," *Mobile Information Systems*, vol. 2017, Article ID 1267608, 13 pages, 2017.
- [34] Y. S. Lee, J. W. Park, and L. Barolli, "A localization algorithm based on AOA for ad-hoc sensor networks," *Mobile Information Systems*, vol. 8, no. 1, pp. 61–72, 2012.
- [35] A. Raimundo, D. Fernandes, D. Gomes, O. Postolache, P. Sebastiao, and F. Cercas, "UAV GNSS position corrections based on IoT™ communication protocol," in *Proceedings of the 2018 International Symposium in Sensing and Instrumentation in IoT Era (ISSI)*, pp. 1–5, Shanghai, China, September 2018.
- [36] Wikipedia, "GNSS applications," 2019, https://en.wikipedia.org/wiki/GNSS_applications.
- [37] S. Ferreira, G. Carvalho, F. Ferreira, and J. Sousa, "Assessing the capacity of man-portable UAVs for network access point localization, using RSSI link data," in *Proceedings of the 2014 International Conference on Unmanned Aircraft Systems (ICUAS)*, pp. 355–364, Orlando, FL, USA, May 2014.
- [38] Wikipedia, "Free-space path loss," 2019, https://en.wikipedia.org/wiki/Free-space_path_loss.
- [39] G. Greco, C. Lucianaz, S. Bertoldo, and M. Allegratti, "Localization of RFID tags for environmental monitoring using UAV," in *Proceedings of the 2015 IEEE 1st International Forum on Research and Technologies for Society and Industry Leveraging a better tomorrow (RTSI)*, pp. 480–483, Turin, Italy, September 2015.
- [40] X. Tian, Z. Song, B. Jiang, Y. Zhang, T. Yu, and X. Wang, "HiQuadLoc: a RSS fingerprinting based indoor localization system for quadrotors," *IEEE Transactions on Mobile Computing*, vol. 16, no. 9, pp. 2545–2559, 2017.
- [41] L. Cheng, C. Wu, Y. Zhang, and a. Y. Wang, "An indoor localization strategy for a mini-UAV in the presence of obstacles," *International Journal of Advanced Robotic Systems*, vol. 9, no. 4, 2017.
- [42] Lowpowerlab, "Moteino Mega," 2019, <https://lowpowerlab.com/shop/product/119>.
- [43] Seeedstudio, "Seeedstudio LoRaWAN," 2016, <https://www.seeedstudio.com/Seeedstudio-LoRaWAN-p-2780.html>.
- [44] Cooking Hacks, "LoRaWAN technology for Arduino, Waspote and raspberry pi," 2019, <https://www.cooking-hacks.com/documentation/tutorials/lorawan-for-arduino-raspberry-pi-waspote-868-900-915-433-mhz>.
- [45] A. Rahmadhani, Richard, R. Isswandhana, A. Giovani, and R. A. Syah, "LoRaWAN as secondary telemetry communication system for drone delivery," in *Proceedings of the 2018*

- IEEE International Conference on Internet of Things and Intelligence System (IOTAIS)*, pp. 116–122, Bali, Indonesia, November 2018.
- [46] T. Salman, “Parameters estimation to achieve distance-based security breaching,” Master thesis, Computer Science and Engineering, Qatar University, Spring, Doha, Qatar, 2015.
 - [47] H. H. R. Sherazi, R. Iqbal, S. U. Hassan, M. H. Chaudary, and S. A. Gilani, “ZigBee’s received signal strength and latency evaluation under varying environments,” *Journal of Computer Networks and Communications*, vol. 2016, Article ID 9409402, 8 pages, 2016.
 - [48] MathsIsFun, “The law of cosines,” 2019, <https://www.mathsisfun.com/algebra/trig-cosine-law.html>.
 - [49] Wikipedia, “True range multilateration,” 2019, https://en.wikipedia.org/wiki/True_range_multilateration.
 - [50] W. Dargie and C. Poellabauer, *Fundamentals of Wireless Sensor Networks*, John Wiley & Sons, Hoboken, NJ, USA, 2010.
 - [51] R. Jin, H. Wang, B. Peng, and N. Ge, “Research on RSSI-based localization in wireless sensor networks,” in *Proceedings of the 2008 4th International Conference on Wireless Communications, Networking and Mobile Computing*, pp. 1–4, Dalian, China, October 2008.
 - [52] O. S. Oguejiofor, A. N. Aniedu, H. C. Ejiofor, and A. U. Okolibe, “Trilateration based localization algorithm for wireless sensor network,” *International Journal of Science and Modern Engineering (IJISME)*, vol. 1, no. 10, 2013.
 - [53] R. Javaid, R. Qureshi, and R. N. Enam, “RSSI based node localization using trilateration in wireless sensor network,” *Bahria University Journal of Information & Communication Technologies*, vol. 8, no. 2, 2015.
 - [54] R. Jain, *The Art of Computer Systems Performance Analysis: Techniques for Experimental Design, Measurement, Simulation, and Modeling*, Wiley Interscience, New York, NY, USA, 1991.
 - [55] M. Wadhwa, M. Song, V. Rali, and S. Shetty, “The impact of antenna orientation on wireless sensor network performance,” in *Proceedings of the 2009 2nd IEEE International Conference on Computer Science and Information Technology*, pp. 143–147, Beijing, China, August 2009.
 - [56] A. Ghubaish, “Locating unmanned aerial vehicles (UAVs),” M.S. thesis, Department of Computer Science and Engineering, Washington University in Saint Louis, Saint Louis, MO, USA, 2017, <https://www.cse.wustl.edu/~jain/theses/agms.htm>.

